

## Fabrication of nanostructured and multicompartimental fabrics based on electrospun nanofibers

Mohammad Kanafchian, Masoomeh Valizadeh, and Akbar Khodaparast Hagh<sup>†</sup>

University of Guilan, P. O. Box 3756, Rasht, Iran  
(Received 19 August 2010 • accepted 7 October 2010)

**Abstract**—The fabrication of novel multilayer electrospun nanofiber web is demonstrated. Under optimized processing conditions, the interface between these webs can be sustained for long time, yielding layers with distinct compartments. Simultaneous control over internal fiber architecture makes these multilayer nano-webs potential candidates for applications such as clothing and industrial filters.

Key words: Electrospun Nanofiber, Nano-web, Nanostructure Fabrics, Laminating, Simulation

### INTRODUCTION

Nowadays, there are different types of protective clothing, some of which are disposable and non-disposable. The simplest and most preliminary of this equipment is made from rubber or plastic that is completely impervious to hazardous substances. Unfortunately, these materials are also impervious to air and water vapor, and thus retain body heat, exposing their wearer to heat stress which can build quite rapidly to a dangerous level. Another approach to protective clothing is incorporating activated carbon into multilayer fabric in order to absorb toxic vapors from environment and prevent penetration to the skin. The use of activated carbon is considered only a short-term solution because it loses its effectiveness upon exposure to sweat and moisture. The use of semi-permeable membranes as a constituent of the protective material is another approach. In this way, reactive chemical decontaminants are encapsulated in micro-particles or fill in microporous hollow fibers and then coats onto fabric. The microparticle or fiber walls are permeable to toxic vapors but impermeable to decontaminants, so that the toxic agents diffuse selectively into them and neutralize [1-3].

Generally, a negative relationship always exists between thermal comfort and protection performance for currently available protective clothing. Thus, there still exists a very real demand for improved protective clothing that can offer acceptable levels of impermeability to highly toxic pollutions of low molecular weight, while minimizing wearer discomfort and heat stress.

Electrospinning provides an ultrathin membrane-like web of extremely fine fibers with very small pore size and high porosity, which makes them excellent candidates for use in filtration, membrane, and possibly protective clothing applications. Preliminary investigations have indicated that the use of nanofiber web in protective clothing structure could present minimal impedance to air permeability and extremely efficiency in trapping dust and aerosol particles. Meanwhile, it is found that the electrospun webs of nylon 6,6, polybenzimidazole, polyacrylonitrile, and polyurethane provided good aerosol particle protection, without a considerable change in

moisture vapor transport or breathability of the system. While nanofiber webs suggest exciting characteristics, it has been reported that they have limited mechanical properties. To provide suitable mechanical properties for use as cloth, nanofiber webs must be laminated via an adhesive into a fabric system. This system could protect ultrathin nanofiber web versus mechanical stresses over an extended period of time [4-6].

The adhesives could be as melt adhesive or solvent-based adhesive. When a melt adhesive is used, the hot-press laminating carried out at temperatures above the softening or melting point of adhesive. If a solvent-based adhesive is used, laminating process could perform at room temperature. In addition, the solvent-based adhesive is generally environmentally unfriendly, more expensive and usually flammable, whereas the hot-melt adhesive is environmentally friendly, inexpensive requires less heat, and so is now more preferred. However, without disclosure of laminating details, the hot-press method is more suitable for nanofiber web lamination. In this method, laminating temperature is one of the most important parameters. Incorrect selection of this parameter may lead to change or damage of nanofiber web. Thus, it is necessary to find a laminating temperature that has the least effect on the nanofiber web.

It has been found that the morphology such as fiber diameter and its uniformity of the electrospun polymer fibers are dependent on many processing parameters. These parameters can be divided into three groups as shown in Table 1. Under certain conditions, not only uniform fibers but also bead-like formed fibers can be produced by electrospinning. Although the parameters of the electrospinning process have been well analyzed in each of polymers, this information

**Table 1. Tensile strength test results of the Multilayer fabrics**

Multilayer fabric	Warp direction			
	Breaking load, N		Breaking elongation, mm	
	Mean value	CV, %	Mean value	CV, %
Without nanofiber web	174.427	6.2	5.02	7.5
With nanofiber web	189.211	4.6	5.11	6

<sup>†</sup>To whom correspondence should be addressed.  
E-mail: Hagh@Guilan.ac.ir

has been inadequate enough to support the electrospinning of ultra-fine nanometer scale polymer fibers. A more systematic parametric study is hence required to investigate.

The purpose of this study is to consider the influence of laminating temperature on nanofiber/laminate properties. Multilayer fabrics were made by electrospinning polyacrylonitrile nanofibers onto non-woven substrate and incorporating into fabric system via hot-press method at different temperatures.

## EXPERIMENTAL

### 1. Electrospinning and Laminating Process

Polyacrylonitrile (PAN) of 70,000 g/mol molecular weight from Polyacryl Co. (Isfahan, Iran) has been used with Dimethylformamide (DMF) from Merck, to form a polymer solution 12% w/w after stirring for 5 h and exposing for 24 h at ambient temperature. The yellow and ripened solution was inserted into a plastic syringe with a stainless steel nozzle 0.4 mm in inner diameter, and then it was placed in a metering pump from WORLD PRECISION INSTRUMENTS (Florida, USA). Next, this set was installed on a plate which it could traverse to left-right along drum (Fig. 1). The flow rate 1  $\mu$ l/h for solution was selected and the fibers were collected on an aluminum-covered rotating drum (with speed 9 m/min) which was previously covered with a polypropylene spun-bond nonwoven (PPSN) substrate of 28 cm  $\times$  28 cm dimensions: 0.19 mm thickness; 25 g/m<sup>2</sup> weight; 824 cm<sup>3</sup>/s/cm<sup>2</sup> air permeability and 140 °C melting point. The distance between the nozzle and the drum was 7 cm and an electric voltage of approximately 11 kV was applied between them. Electrospinning process was carried out for 8 h at room temperature to reach approximately web thickness 3.82 g/m. Then nanofiber webs were laminated into cotton weft-warp fabric with a thickness 0.24 mm and density of 25  $\times$  25 (warp-weft) per centimeter to form a multilayer fabric (Fig. 2). Laminating was performed at temperatures 85, 110, 120, 140, 150 °C for 1 min under a pressure of 9 g/cm<sup>2</sup>.

### 2. Nanofiber Web Morphology

To consider nanofiber web morphology after hot-pressing, another laminating was performed by a non-stick sheet made of Teflon (0.25 mm thickness) instead one of the fabrics (fabric/PP web/nanofiber web/PP web/non-stick sheet). Finally, after removing of Teflon sheet, the nanofiber layer side was observed under an optical microscope

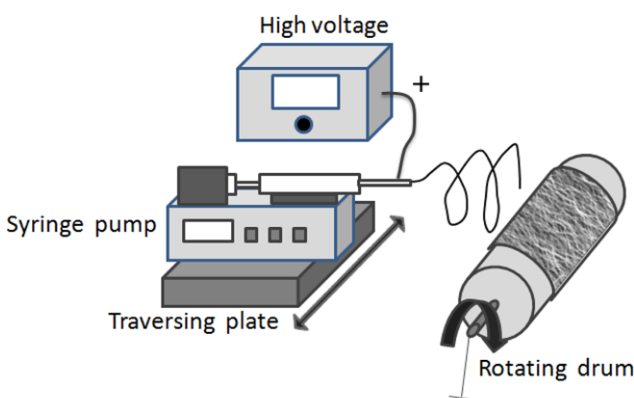


Fig. 1. Electrospinning setup.

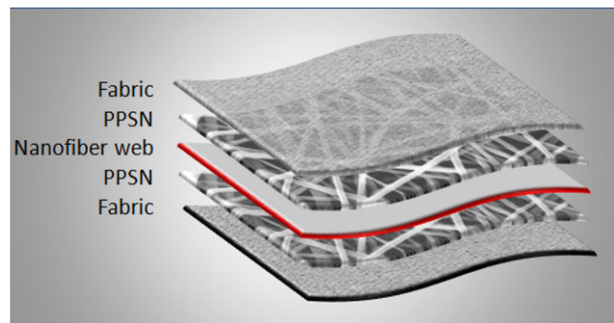


Fig. 2. Multilayer fabric components.

(MICROPHOT-FXA, Nikon, Japan) connected to a digital camera.

### 3. Measurement of Air Permeability

Air permeability of multilayer fabric after lamination was tested by TEXTEST FX3300 instrument (Zürich, Switzerland). Five pieces of each sample were tested under air pressure 125 pa at ambient condition (16 °C, 70%RH) and average air permeability was obtained.

### 4. Mechanical Properties of Multilayer Nano-web

The tensile strength of multilayer fabrics with and without nanofiber web, were carried out using MICRO250 tensile machine (SDL International Ltd.). Ten samples were cut from the warp directions of multilayer fabric at size of 10 mm  $\times$  200 mm and then exposed to the standard condition (25 °C, 60% RH) for 24 h in order to do conditioning. To measure tensile strength, testing was performed by load cell of 25 Kgf. Also, the distance between the jaws and the rate of extension were selected 100 mm and 20 mm/min, respectively.

## RESULTS AND DISCUSSION

PPSN was selected as melt adhesive layer for hot-press laminating (Fig. 2). This process was performed under different temperatures to find an optimum condition. Fig. 3 presents the optical microscope images of nanofiber web after lamination. It is obvious that by increasing of laminating temperature to melting point (samples a-c), the adhesive layer gradually melts and spreads on the web surface. But, when melting point was selected as laminating temperature (sample d) the nanofiber web began to be damaged. In this case, the adhesive layer completely melted and penetrated into nanofiber web and occupied its pores. This procedure intensified by increasing of laminating temperature above the melting point. As shown in Fig. 1 (sample e), perfect absorption of adhesive by nanofiber web creates a transparent film which leads to fabric structure appearing.

### 1. Breathability

Also, to examine how laminating temperature affects the breathability of multilayer fabric, an air permeability experiment was performed. Fig. 4 indicates the effect of laminating temperature on air permeability. As might be expected, air permeability decreased with increasing laminating temperature; this behavior is attributed to the melting procedure of the adhesive layer. As mentioned above, before the melting point the adhesive gradually spreads on the web surface. This phenomenon causes the adhesive layer to act like an impervious barrier to air flow and reduces air permeability of multilayer fabrics. But at the melting point and above, the penetration of melt adhesive into nanofiber/fabric structure leads to filling its pores and

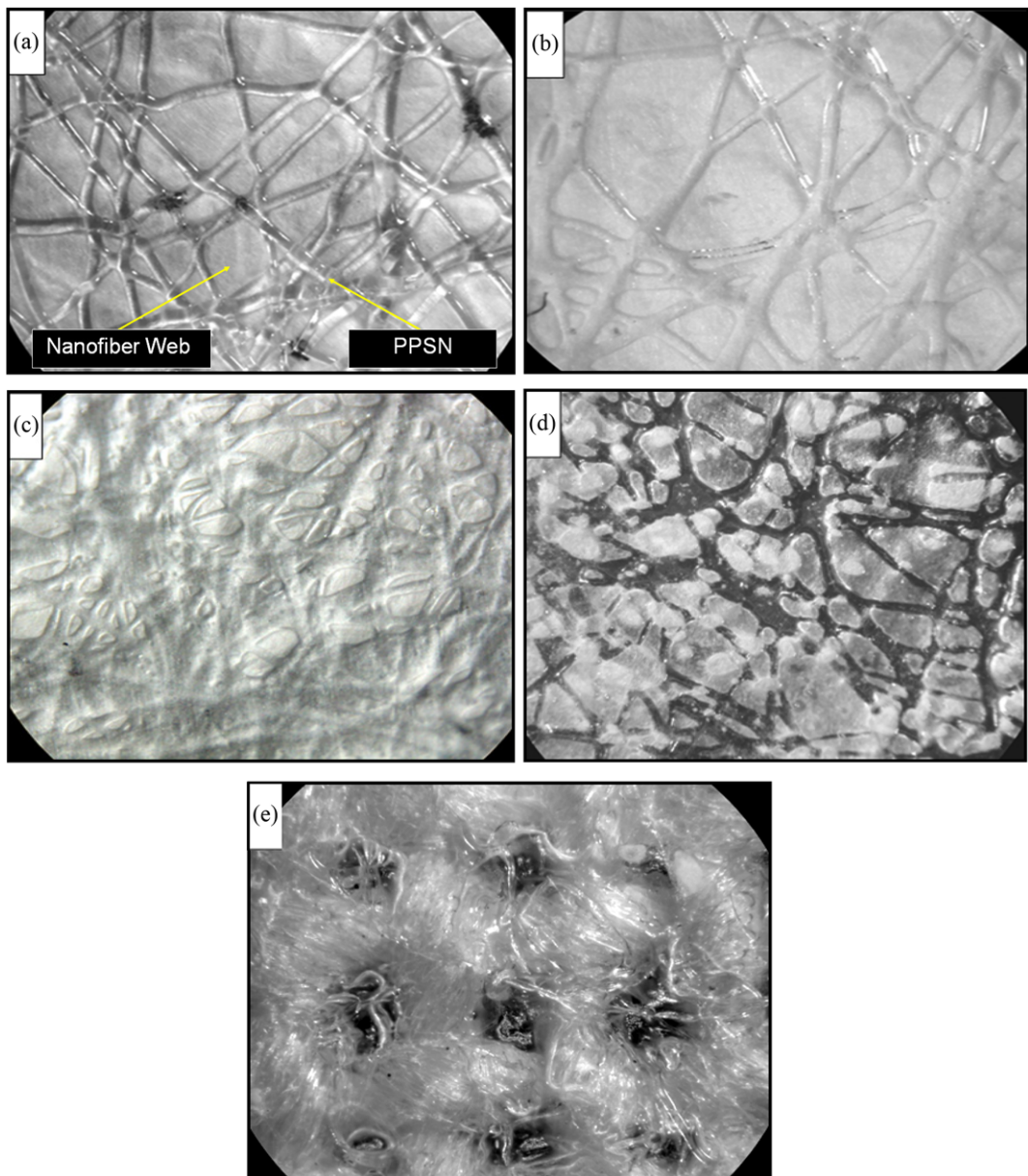


**Fig. 3.** (a) The optical microscope images of nanofiber web after laminating at 85 °C (at 100 magnification). (b) The optical microscope images of nanofiber web after laminating at 110 °C (at 100 magnification). (c) The optical microscope images of nanofiber web after laminating at 120 °C (at 100 magnification). (d) The optical microscope images of nanofiber web after laminating at 140 °C (at 100 magnification). (e) The optical microscope images of nanofiber web after laminating at temperatures more than 140 °C (at 100 magnification).

finally decreasing air permeability.

## 2. Adhesion of Layers

Furthermore, we only observed that the adhesive force between layers was increased according to temperature rise. Sample (a) exhibited very poor adhesion between nanofiber web and fabric and it could be separated by light abrasion of thumb, while adhesion increased by increasing laminating temperature to melting point. It must be noted that after the melting point because of passing of melt PPSN across nanofiber web, adhesion between two layers of fabric will occur.

## 3. Tensile Strength

The tensile strength of samples without nanofibers (Fig. 5) is weaker

than those laminated with nanofibers (Fig. 6). According to Table 2, the breaking load and breaking elongation for the samples laminated with electrospun nanofibers are improved as well. These variations can be observed clearly in Figs. 7 and 8 for 10 samples.

## 4. Simulation of Nano-web

For the continuous fibers, it is assumed that the lines are infinitely long so that in the image plane, all lines intersect the boundaries. Under this scheme (Fig. 9), a line with a specified thickness is defined by the perpendicular distance  $d$  from a fixed reference point  $O$  located in the center of the image and the angular position of the perpendicular  $\alpha$ . Distance  $d$  is limited to the diagonal of the image.

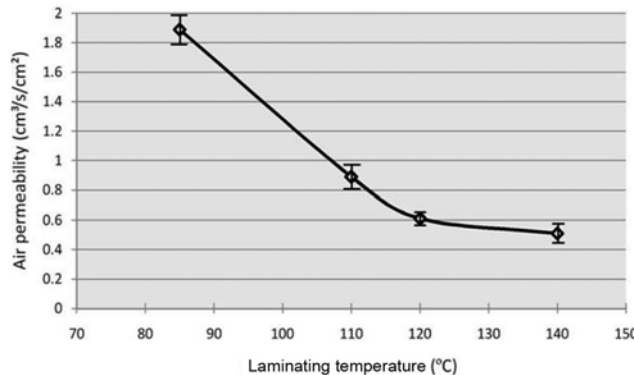


Fig. 4. Air permeability of multilayer fabric as a function of laminating temperature.

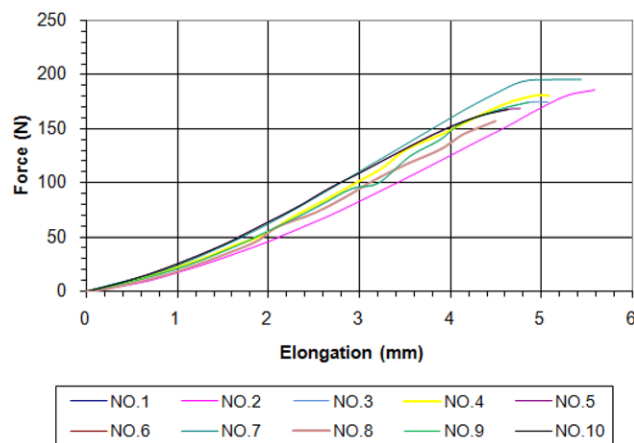


Fig. 5. Force-Elongation curve for multilayer fabric without nanofiber web.

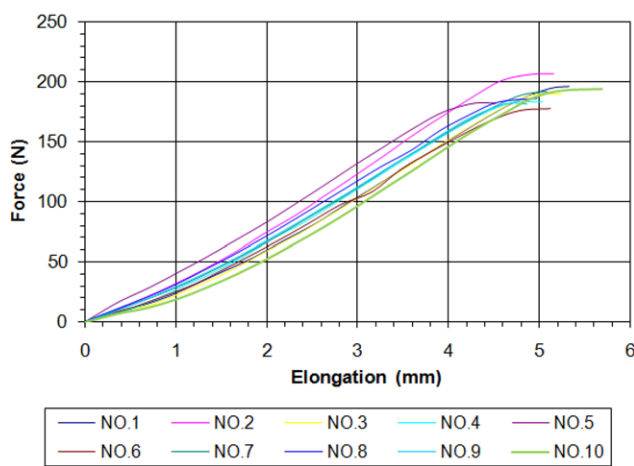


Fig. 6. Force-Elongation curve for multilayer fabric with nanofiber web.

Based on the objective of this paper, several variables are allowed to be controlled during the simulation:

1. *Web density* can be controlled by using the line density which is the number of lines to be generated in the image.

2. *Angular density* is useful for generating fibrous structures with

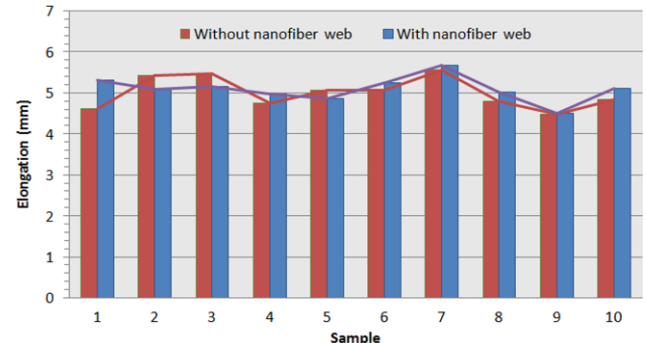


Fig. 7. Breaking elongation of ten samples.

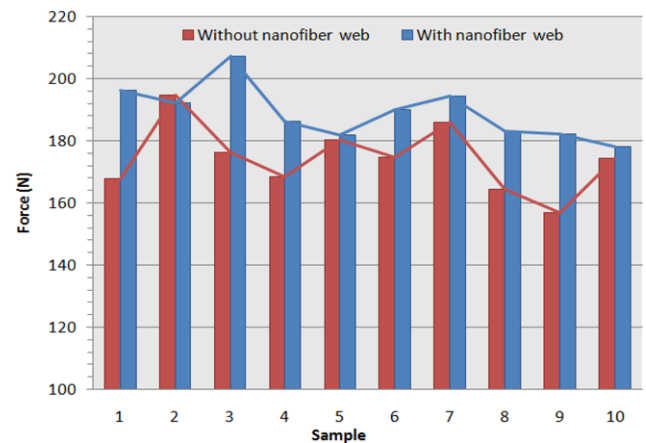


Fig. 8. Breaking load of ten samples.

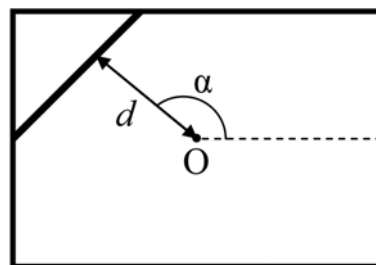


Fig. 9. Procedure for  $\mu$ -randomness.

specific orientation distribution. The orientation may be sampled from either a normal or a uniform random distribution.

3. *Distance from the reference point* normally varies between zero and the diagonal of the image, restricted by the boundary of the image and is sampled from a uniform random distribution.

4. *Line thickness* (fiber diameter) is sampled from a normal distribution. The mean diameter and its standard deviation are needed.

5. *Image size* can also be chosen as required.

## 5. Fiber Diameter Measurement

The first step in determining fiber diameter is to produce a high quality image of the web, called a micrograph, at a suitable magnification using electron microscopy techniques. The methods for measuring electrospun fiber diameter are described in the following sections.

## 6. Manual Method

The conventional method of measuring the fiber diameter of elec-

trospun webs is to analyze the micrograph manually. The manual analysis usually consists of determining the length of a pixel of the image (setting the scale), identifying the edges of the fibers in the image and counting the number of pixels between two edges of the fiber (the measurements are made perpendicular to the direction of fiber-axis), converting the number of pixels to nm using the scale and recording the result. Typically, 100 measurements are performed (Fig. 10).

However, this process is tedious and time-consuming, especially for a large number of samples. Furthermore, it cannot be used as

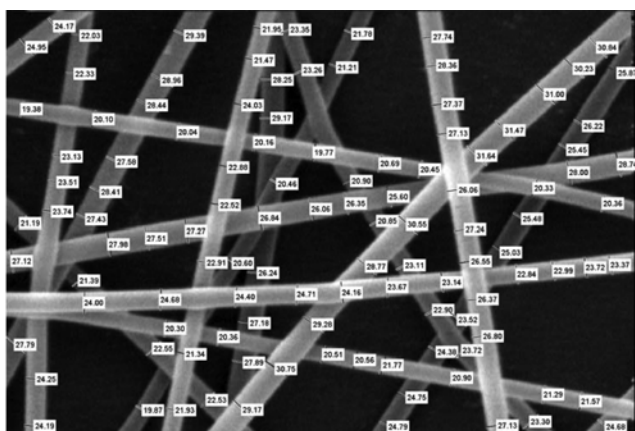


Fig. 10. Manual method.

an on-line method for quality control since an operator is needed for performing the measurements. Thus, developing automated techniques which eliminate the use of an operator and have the capability of being employed as on-line quality control is of great importance.

### 7. Distance Transform

The *distance transform* of a binary image is the distance from every pixel to the nearest nonzero-valued pixel. The center of an object in the distance transformed image will have the highest value and lie exactly over the object's *skeleton*. The skeleton of the object can be obtained by the process of *skeletonization* or *thinning*. The algorithm removes pixels on the boundaries of objects but does not allow objects to break apart. This reduces a thick object to its corresponding object with one pixel width. Skeletonization or thinning often produces short spurs which can be cleaned up automatically with a *pruning* procedure.

The algorithm for determining fiber diameter uses a binary input image and creates its skeleton and distance transformed image. The skeleton acts as a guide for tracking the distance transformed image by recording the intensities to compute the diameter at all points along the skeleton. Fig. 11 shows a simple simulated image, which consists of five fibers with diameters of 10, 13, 16, 19 and 21 pixels, together with its skeleton and distance map including the histogram of fiber diameter obtained by this method.

### 8. Direct Tracking

Direct tracking method uses a binary image as an input data to determine fiber diameter based on information acquired from two

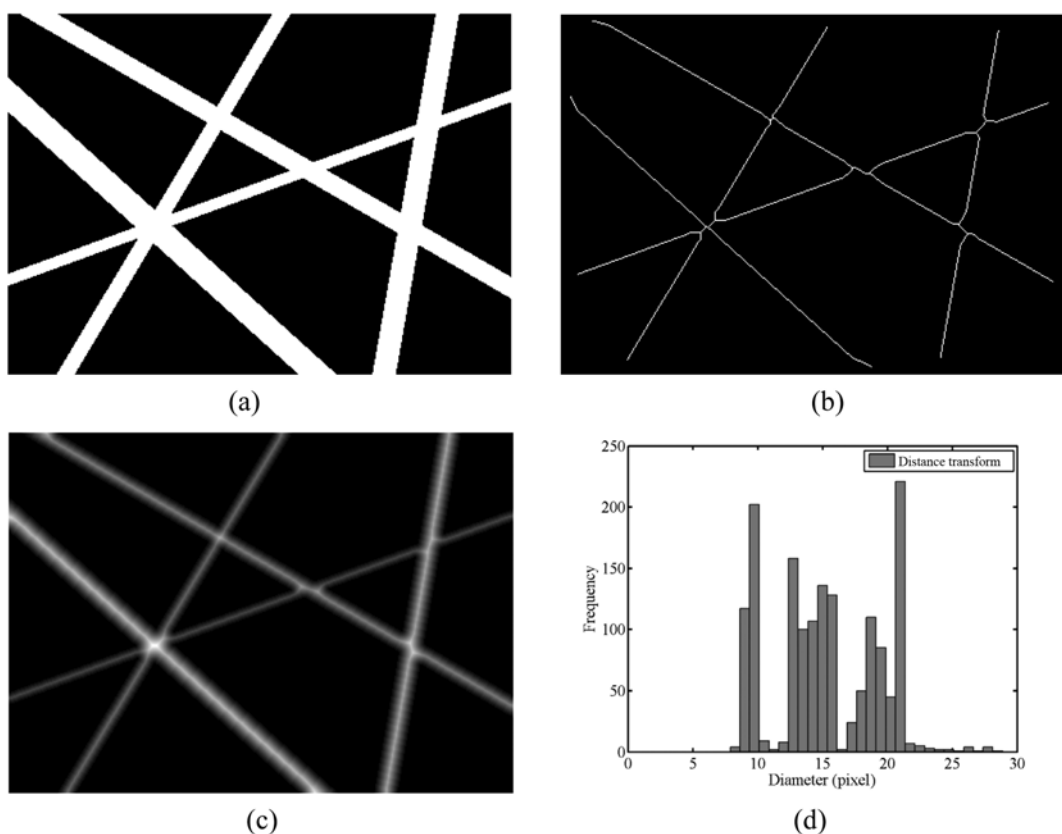


Fig. 11. (a) A simple simulated image, (b) Skeleton of (a), (c) Distance map of (a) after pruning, (d) Histogram of fiber diameter distribution obtained by distance transform method.

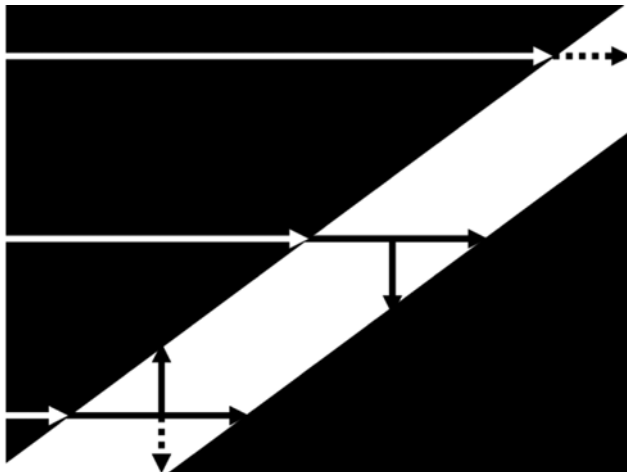


Fig. 12. Diameter measurement based on two scans in direct tracking method.

scans: first a horizontal and then a vertical scan. In the horizontal scan, the algorithm searches for the first white pixel adjacent to a black. Pixels are counted until the first black is reached. The second scan is then started from the midpoint of the horizontal scan and pixels are counted until the first black is encountered. Direction changes if the black pixel isn't found. Having the number of horizontal and vertical scans, the number of pixels in perpendicular direction, which is the fiber diameter, could be measured from a geometrical relationship. The explained process is illustrated in Fig. 12.

In electrospun nonwoven webs, nanofibers cross each other at intersection points, which brings about the possibility for some untrue measurements of fiber diameter in these regions. To circumvent this problem, a process called *fiber identification* is employed. First, black regions are labeled and couple of regions between which a fiber exists are selected. In the next step, the two selected regions are connected by performing a *dilation* operation with a large enough *structuring element*. Dilation is an operation that grows or thickens objects in a binary image by adding pixels to the boundaries of objects. The specific manner and extent of this thickening is controlled by the size and shape of the structuring element used. In the following process, an *erosion* operation with the same structuring element is

performed and the fiber is recognized. Erosion shrinks or thins objects in a binary image by removing pixels on object boundaries. As in dilation, the manner and extent of shrinking is controlled by a structuring element. Then, in order to enhance the processing speed, the image is cropped to the size of selected regions. Afterwards, fiber diameter is measured according to the previously explained algorithm. This trend is continued until all of the fibers are analyzed. Finally, the data in pixels may be converted to  $nm$  and the histogram of fiber diameter distribution is plotted. Fig. 13 shows a labeled simple simulated image and the histogram of fiber diameter obtained by this method.

## CONCLUSION

The effect of laminating temperature on nanofiber/laminate properties was investigated to make next-generation protective clothing. First, surface images of nanofiber web after lamination were taken with an optical microscope in order to consider morphology changes. It was observed that the nanofiber web remained unchanged as laminating temperature was below PPSN melting point. In addition, to compare breathability of laminates, air permeability was measured. It was found that by increasing laminating temperature, air permeability was decreased. Furthermore, it only was observed that the adhesive force between layers in laminate was increased with temperature rise. The mechanical properties of the samples laminated by electrospun nanofibers showed significant improvements.

These results indicate that laminating temperature is an effective parameter for lamination of nanofiber web into fabric structure. Thus by varying this parameter, fabrics could be developed with different levels of thermal comfort and protection depending on our need and use.

## REFERENCES

1. H. Fong and D. H. Reneker, *Electrospinning and the formation of nanofibers*, in: D. R. Salem (Ed.), *Structure formation in polymeric fibers*, Hanser, Cincinnati (2001).
2. D. Li and Y. Xia, *Adv. Mater.*, **16**, 1151 (2004).
3. R. Derch, A. Greiner and J. H. Wendorff, *Polymer nanofibers pre-*

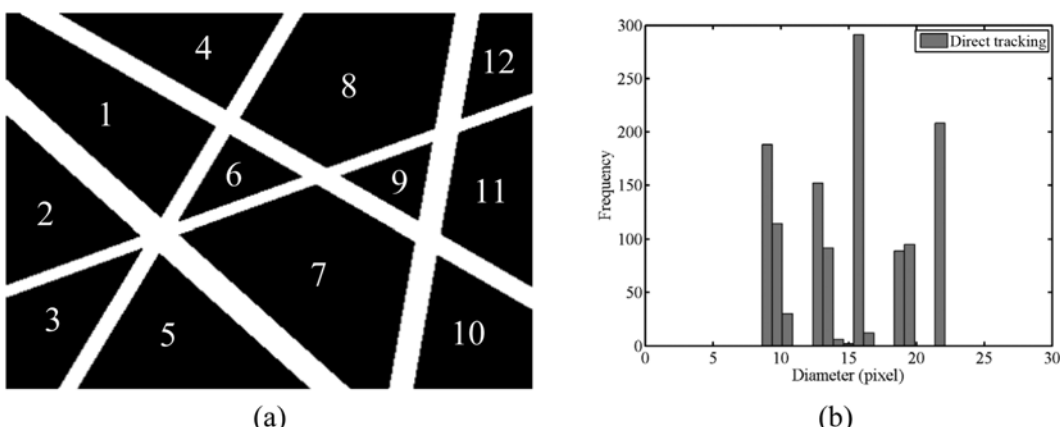


Fig. 13. (a) A simple simulated image which is labeled, (b) Histogram of fiber diameter distribution obtained by direct tracking.

pared by electrospinning, in: J. A. Schwarz, C. I. Contescu and K. Putyera (Eds.), *Dekker encyclopedia of nanoscience and nanotechnology*, CRC, New York (2004).

4. M. Ziabari, V. Mottaghitalab and A. K. Haghi, *Korean J. Chem. Eng.*, **25**(4), 919 (2008).

5. M. Ziabari, V. Mottaghitalab and A. K. Haghi, *Korean J. Chem. Eng.*, **25**(4), 923 (2008).

6. M. Ziabari, V. Mottaghitalab and A. K. Haghi, *Korean J. Chem. Eng.*, **25**(4), 905 (2008).